DALTON

Structural characterization of spherical octadecavanadates encapsulating Cl^- and H_2O†

Toshihiro Yamase,* Kawori Ohtaka and Masamichi Suzuki

Research Laboratory of Resources Utilization, Tokyo Institute of Technology, 4259 Nagatsuta, Midori-ku, Yokohama 226, Japan

Spherical octadecavanadate complexes $K_{9.5}[H_{3.5}V_{18}O_{42}Cl]\cdot 11.5H_2O$ **1** and $K_{10}[H_2V_{18}O_{42}(H_2O)]\cdot 16H_2O$ **2** have been photochemically prepared by self-assembly of the components in solution under ambient conditions, and characterized by elemental analyses, IR spectra, crystal structure determinations and magnetic susceptibility measurements. They consist of $(VO)_{18}O_{24}$ shells encapsulating Cl^- and H_2O at the centre, respectively. Each shell is composed of eighteen edge-sharing $V^{IV}O_5$ square pyramids and has approximate D_{4d} symmetry. The inner diameter of the shell is 0.1–0.2 Å smaller for **1** than for **2**. This can be explained by the electrostatic attraction between V^{IV} and Cl^- which results in shorter $V^{IV}\cdots V^{IV}$ distances due to weakening of the electrostatic repulsion between V^{IV} atoms, and is reflected in both the IR spectra and magnetic properties. The V–O–V vibrational stretching modes for **1** are shifted to slightly higher wavenumbers. The magnetic susceptibility, which shows a strong coupling within the $V^{IV}\cdots V^{IV}$ pairs in the two anions which leaves six to four V^{IV} atoms uncoupled at $50 \leqslant T \leqslant 300$, is also slightly higher for **1**.

We have reported that the photolysis of aqueous solutions containing $[V_4O_{12}]^{4-}$ and alcohols at pH 9 (adjusted with K_2CO_3) leads to the formation of the CO_3^{2-}-included mixed-valence cluster $[V_{15}O_{36}(CO_3)]^{7-}$, as a result of electron transfer from the alcohols into the O→V ligand-to-metal charge-transfer (l.m.c.t.) excited triplet states of $[V_4O_{12}]^{4-}$.[1] Similar $[V_{15}O_{36}X]^{n-}$ clusters encapsulating X = Cl^-, Br^-, PO_3^- and NO_3^- were synthesized by prolonged photolysis of aqueous solutions containing Na_3VO_4 and alcohols at pH 8–10 adjusted with HCl, HBr, H_3PO_3 and HNO_3, respectively. The clusters $[V_{15}O_{36}(CO_3)]^{7-}$ and $[V_{15}O_{36}Br]^{6-}$ have also been prepared using the thermal reactions of V_2O_5, Li_2CO_3 and $[H_2NNH_3]_2[SO_4]$ at 90 °C and NMe_4Br and $[NH_4]_3[VS_4]$ at 60–65 °C.[2]

Our interest lies in the photochemical design of the structure of isopolyoxovanadate clusters which are new classes of spherical cluster shell serving as hosts for neutral and charged species with vastly different cavity requirements, *e.g.* $[V_{12}O_{32}(MeCN)]^{4-}$, $[H_9V_{18}O_{46}(VO_4)]^{8-}$ {= $[V_{18}O_{37}(OH)_9(VO_4)]^{8-}$}, $[V_{15}O_{36}X]^{6-}$ (X = Cl or Br), $[HV_{22}O_{54}(ClO_4)]^{6-}$ {= $[V_{22}O_{53}(OH)(ClO_4)]^{6-}$}, $[H_4V_{18}O_{42}Br]^{9-}$, $[H_2V_{18}O_{44}(N_3)]^{5-}$ {= $[V_{18}O_{42}(OH)_2(N_3)]^{5-}$} and $[V_{34}O_{82}]^{10-}$ (= $[\{(V^{IV}{}_4O_4)O_4\}(V_{30}O_{74})]^{10-}$).[2–7] Although the mechanism of the preferential formation of encapsulating polyoxovanadates is not at all clear, the structure of the spherical isopolyoxovanadate shells formed *via* self-organization seems to be governed by a variety of starting vanadates, reducing agents, anionic reagents for the molecular recognition (templates) and solution pH. We recently found photochemical formation of V_{18} clusters exemplified by $[V^{IV}{}_{18}O_{42}Cl]^{13-}$ and $[V^{IV}{}_{18}O_{42}(H_2O)]^{12-}$: the addition of KCl to the brown photolyte obtained by photoredox reaction of $[V_4O_{12}]^{4-}$ with MeOH at pH 9.5 (adjusted with KOH) yields $K_{9.5}[H_{3.5}V_{18}O_{42}Cl]\cdot 11.5H_2O$ **1**, while photolysis of $[VO_4]^{3-}$ in the presence of MeOH at pH 14 (adjusted with KOH) provides $K_{10}[H_2V_{18}O_{42}(H_2O)]\cdot 16H_2O$ **2**. This suggests an adaptability of the structural variety of the spherical cluster shell in the photochemistry of polyoxovanadates. So far, crystalline Cl^-- and H_2O-encapsulated octadecavanadates, $K_9[H_4V^{IV}{}_{18}O_{42}Cl]\cdot 6H_2O$ and $K_{12}[V^{IV}{}_{18}O_{42}]\cdot 16H_2O$, have also been prepared by thermal reactions of KVO_3 with hydrazinium hydroxide at 90–95 °C in aqueous solution at pH 8 adjusted with HCl (for the Cl^--inclusion cluster) and $VOSO_4$ with KOH at 60–70 °C in aqueous solution at pH 14 (for the H_2O-inclusion cluster), respectively. However, the crystal structure of the former has not been determined probably due to its low stability, in contrast with $Cs_9[H_4V^{IV}{}_{18}O_{42}Br]\cdot 12H_2O$ for which a complete X-ray crystallographic characterization has been reported.[2] In $K_{12}[V^{IV}{}_{18}O_{42}]\cdot 16H_2O$, the positions of two K^+ and five H_2O could not be determined because of disorder. Furthermore, the above encapsulated-H_2O species could not be unequivocally identified.[8] For this point of view we investigated the crystal structures of clusters **1** and **2** prepared photochemically. We describe herein their preparation and characterization, for a better understanding of the properties of V_{18} clusters formed *via* spontaneous self-assembly in photolytes under ambient conditions.

Experimental

Materials, preparations and measurements

All the reagents were of at least analytical grade and used without further purification. The salt $[NH_3Bu^t]_4[V_4O_{12}]$ was synthesized according to the published procedure and identified in the solid state by comparison of the IR spectrum with that previously reported.[9] The cluster $K_{9.5}[H_{3.5}V_{18}O_{42}Cl]\cdot 11.5H_2O$ **1** was prepared as follows: $[NH_3Bu^t]_4[V_4O_{12}]$ (0.4 g, 0.6 mmol) was dissolved in water (20 cm^3) in a Pyrex tube (20 cm^3), to give pH 6.8. The mixture was adjusted to pH 9.5 with KOH and MeOH (2 cm^3) was added. The resulting solution was irradiated for 9 h under an atmosphere of nitrogen using a 500 W superhigh-pressure mercury lamp. Saturated aqueous KCl solution (2 cm^3) was added to the dark brown photolyte to yield 0.15 g of **1**. Dark brown single rhombic crystals were precipitated within 1 d after addition of KCl to the photolyte. The cluster $K_{10}[H_2V_{18}O_{42}(H_2O)]\cdot 16H_2O$ **2** was prepared similarly: an aqueous solution (20 cm^3) containing $[NH_3Bu^t]_4[V_4O_{12}]$ (0.5 g, 0.7 mmol) was adjusted to pH 14 with KOH and then MeOH (2 cm^3) was added. Photolysis of the resulting solution for 1 d provided brown single rod-like crystals with a yield of 0.2 g. Crystalline **2** was also prepared by

† Photochemistry of Polyoxovanadates. Part 2.[1]

Non-SI units employed: $\mu_B \approx 9.27 \times 10^{-24}$ J T^{-1}; emu = $4\pi \times 10^{-6}$ cm^3.

adjusting the above dark brown photolyte (at pH 9.5) to pH 13.5 with KOH.

Analysis of V^{IV} and V^{V} in the samples was made by potentiometric titration under an atmosphere of nitrogen; the potential of a platinum indicator electrode *vs.* a Ag–AgCl reference electrode at open circuit was measured by a TOA Electronics IM-5S ion meter. The number of vanadium(IV) centres was unambiguously established by back titration analysis: a known excess of $KMnO_4$ was added to the sample in 1 mol dm^{-3} H_2SO_4 to oxidize V^{IV} to V^{V} which was determined using a standard solution of ammonium iron(II) sulfate. Back titrations of **1** and **2** gave average vanadium oxidation states of 4.06 ± 0.03 and 4.04 ± 0.01, respectively. Potassium was determined potentiometrically by use of a TOA Electronics IM-5S ion meter. Thermogravimetric analysis using a Rigaku Thermoflex TG-DGC instrument was used for the determination of lattice water (Found: Cl, 1.85; K, 17.30; V, 40.40. Calc. for $H_{26.5}ClK_{9.5}O_{53.5}V_{18}$: Cl, 1.60; K, 16.85; V, 41.55. Found: K, 16.65; V, 38.80. Calc. for $H_{36}K_{10}O_{59}V_{18}$: K, 17.10; V, 40.10%). Other V_{18} clusters encapsulating other anions such as Br^-, I^- and NO_3^- were similarly synthesized by modification of the procedure for **1**.

The IR and X-band ESR spectra were recorded on JASCO FT/IR-5000 and JEOL X-band RE1X spectrometers, respectively. The magnetic measurements were carried out on microcrystalline samples with a magnetometer (Quantum design, MPMS-5S) equipped with a SQUID sensor. The temperature range was 4–300 K, and the magnetic field was 1.0 T. The molar susceptibility was corrected for the diamagnetic contributions of clusters **1** and **2** (-913×10^{-6} and -964×10^{-6} emu, respectively) using standard Pascal constants.[10]

X-Ray structural analysis

Crystals were sealed in Lindemann glass capillaries and mounted on a Rigaku AFC-5 diffractometer equipped with graphite crystal-monochromatized Mo-Kα (λ = 0.710 69 Å) radiation. The intensities were collected by ω–2θ scans at a 2θ scan rate of 8° min^{-1} at room temperature. The orientation matrix and cell dimensions were obtained from the setting angles of 24 centred reflections in the range 22.1–24.9 and 15.1–18.9° for clusters **1** and **2**, respectively. No significant decay in intensity of three standard reflections recorded after every 100 was observed. The vanadium positions were determined by a direct method using MITHRIL;[11] K, O and Cl atoms were located from difference syntheses. Lorentz and polarization factors were applied and an absorption correction was made based on the isotropically refined structure, using the program DIFABS.[12] The correction factors were 0.77–1.28 and 0.33–1.74 for **1** and **2**, respectively. Subsequently for **1** the V, Cl and K atoms were refined with anisotropic thermal parameters and for **2** the V, oxide O and K atoms. Refinements on $|F_o|$ for all non-H atoms were carried out using the full-matrix least-squares method. The quantity minimized was $\Sigma w(|F_o| - |F_c|)^2$. Attempts were made to refine potassium and crystal-water oxygen atoms, with various combinations of site occupancy factors. A summary of crystal data for **1** and **2** is shown in Table 1. The weighting scheme employed was $w^{-1} = \sigma^2(F_o)$, where $\sigma^2(I_o) = \sigma^2(I_{counting}) + (0.038I_o)^2$ and $\sigma^2(I_o) = \sigma^2(I_{counting}) + (0.043I_o)^2$ for **1** and **2**, respectively. The maximum and minimum heights in the final difference synthesis were 2.3 (1.7) and -1.4 e $Å^{-3}$ in **1** (-1.5 in **2**), respectively. All calculations were carried out on a Micro VAX II computer using the TEXSAN software package.[13]

Complete atomic coordinates, thermal parameters and bond lengths and angles have been deposited at the Cambridge Crystallographic Data Centre. See Instructions for Authors, *J. Chem. Soc., Dalton Trans.*, 1996, Issue 1.

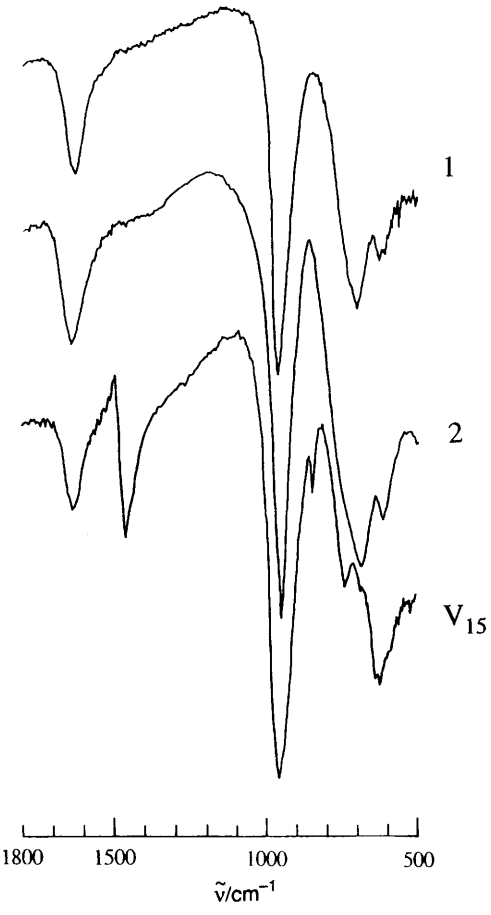

Fig. 1 Infrared spectra of clusters **1**, **2** and $K_5[H_2V_{15}O_{36}(CO_3)]\cdot14.5H_2O$

Results and Discussion

Infrared spectra of clusters 1 and 2

A selected region of the IR spectra of $K_{9.5}[H_{3.5}V_{18}O_{42}Cl]\cdot11.5H_2O$ **1** and $K_{10}[H_2V_{18}O_{42}(H_2O)]\cdot16H_2O$ **2** is shown in Fig. 1 together with the spectrum of $K_5[H_2V_{15}O_{36}(CO_3)]\cdot14.5H_2O$[1] for comparison. Clusters **1** and **2** in KBr discs exhibit bands around 1630m (1631 ± 1 for **1** and 1630 ± 1 for **2**), 956s (957 ± 2 and 954 ± 2), 700s (703 ± 1 and 696 ± 1) and 625m (626 ± 1 and 621 ± 1) cm^{-1}. The strong broad band around 956 cm^{-1} is due to V–O stretching of the spherical cluster shell formed by linking VO_5 pyramids (as shown below) and the feature at 700–600 cm^{-1} is attributed to symmetric and asymmetric V–O–V stretchings. The V–O–V stretching bands for **1** appear slightly to high energy compared with those for **2**. The comparison between the V_{15} and V_{18} clusters shows that the existence of two bands around 1460 and 845 cm^{-1} is the best evidence of the V_{15} cluster, as was mentioned previously.[1]

Crystal structures

The anions in clusters **1** and **2** are $V_{18}O_{42}$ shells constructed by eighteen VO_5 square pyramids, encapsulating Cl^- and H_2O, respectively. The H_2O molecule at the centre of the anion in **2** was statistically disordered, as the positions of the water H atoms could not be observed in Fourier-difference maps. Atomic coordinates are listed in Table 2. The unit cells for **1** and **2** contain two and four molecules, respectively. The X-ray structural analyses of **1** and **2** formally reveal the encapsulation of Cl and water O(43) atoms, respectively, at the centre of the anion. Ten K^+ cations are identified for each isopolyoxovanadate anion. Since in **1** one K atom [K(1)] is situated at a crystallographic centre of symmetry, **1** contains 9.5 K^+ cations. The average vanadium oxidation state of +4, obtained by the

potentiometric analysis, indicates that the anions of **1** and **2** are fully reduced. Thus, it is reasonable to formulate **1** and **2** as $K_{9.5}[H_{3.5}V_{18}O_{42}Cl]\cdot 11.5H_2O$ and $K_{10}[H_2V_{18}O_{42}(H_2O)]\cdot 16H_2O$ respectively, in order to maintain electrical neutrality.

Although the anion cages in clusters **1** and **2** are almost identical, there are slight differences in bond lengths and angles attributed to effects of the encapsulated species and packing in the lattice. The anion structure is exemplified for **1** in Fig. 2. Stereoscopic drawings of the anions in **1** and **2** are shown in Fig. 3(*a*) and 3(*b*), respectively. The anions have approximate D_{4d} symmetry, which gives an S_8 axis through V(1)–Cl–V(2) in **1** and V(1)–O(43)–V(2) in **2**. The V=O bond lengths range from 1.58(1) to 1.66(1) Å. All of the twenty-four oxygen atoms of the anion bridge three V atoms with bond lengths of 1.86(1)–2.01(1) Å, resulting in the generation of a $(VO)_{18}O_{24}$ spherical shell. For each μ_3-O(19–42) atom the V–O–V angles fall in two distinct groups: (1) *ca.* 145° [140.0(6)–148.7(7) in **1** and 142.5(8)–150.2(8)° in **2**] and (2) *ca.* 100° [93.2(6)–102.0(6) in **1** and 96.6(6)–101.7(6)° in **2**]. The relative values of the terminal V=O bond strengths $(d/1.770)^{-5.2}$, where d is the bond length in Å,[14] are 1.4(1)–1.8(2). The values for some of the terminal oxygen atoms are smaller compared with those of the μ_3-O oxygen atoms [(1.8(2)–1.9(2)], implying the population of significant negative charge on the terminal O atoms if they are not protonated. Since the OH^- oxygen atom displays a Lewis-base strength of 1.2 assuming two-co-ordination,[15] it is likely that the protons in the anions for **1** and **2** are distributed on some of the terminal O atoms. In **1** the Cl or in **2** the O(43) atom in the central cavity of the anion interacts due to weak repulsive forces with twenty-four oxygen atoms [O(19)–O(42)] at an average distance of 3.67(3) Å [3.58(1)–3.82(1) in **1** and 3.57(3)–3.77(3) Å in **2**]. The separations between the central Cl (in **1**) or O(43) (in **2**) and the positively charged vanadium [V(1)–V(18)] centres are also large, average 3.751(8) [3.592(8)–3.952(8)] in **1** and 3.80(3) Å [3.70(3)–3.94(2)] in **2**. Such large separations from V(1)–V(18) and μ_3-O(19–42) atoms suggest co-ordination numbers as high as 42. The large co-ordination sphere of the central atom indicates that the central Cl^- and H_2O will be readily replaced by other anions. Thus, the fact that crystalline **1** was obtained by the addition of KCl to the photolyte from $[V_4O_{12}]^{4-}$–MeOH–KOH (pH 9.5), which provided crystalline **2** on change to pH 13.5, suggests that the central H_2O molecule in the V_{18} cluster is replaced by Cl^- at pH 9.5. It is noteworthy that the average Cl···V distance in **1** is slightly shorter than the average O(43)···V distance (in **2**) which is similar to the average (3.75 Å) I···V distance (3.68–3.86 Å) in $Cs_9[H_4V_{18}O_{42}I]\cdot 12H_2O$ (encapsulated I^- with a large effective ionic radius of 2.20 Å).[2] The structurally compact nature of **1** originates from the electrostatic attraction between the negative Cl^- and positive V^{IV}. The alternative possibility that OH^- could be encapsulated in the $V_{18}O_{42}$ cage in strongly alkaline (pH 13.5) solutions is unlikely, since the effective ionic radii of O^{2-} (1.35 Å) and Cl^- (1.81 Å)[16] would make the O(43)···V distances (in **2**) much shorter than the Cl···V distances.

If a maximum K–O distance of 3.5 Å is assumed, the K^+ cations occupy positions between the anions with irregular seven- to nine-co-ordination by oxygen atoms. In cluster **1** the site occupancy of a lattice water oxygen atom O(52) was fixed at 0.5 throughout the structure refinement since the short distance [1.70(8) Å] of O(52)···O(52$^{\bar{X}}$) (symmetry relation $\bar{X}$ $1-x, -y, -1-z$) may be brought about by the disordered structure of the O(52) atom. The cations and water molecules serve to bind the anions together by a complex system of ionic and hydrogen bonds.

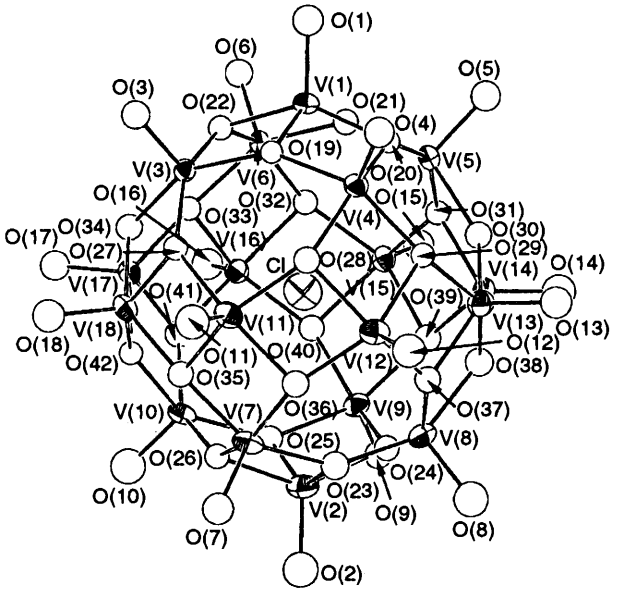

Fig. 2 Schematic representation of the structure of $[V_{18}O_{42}Cl]^{13-}$ with atom labelling

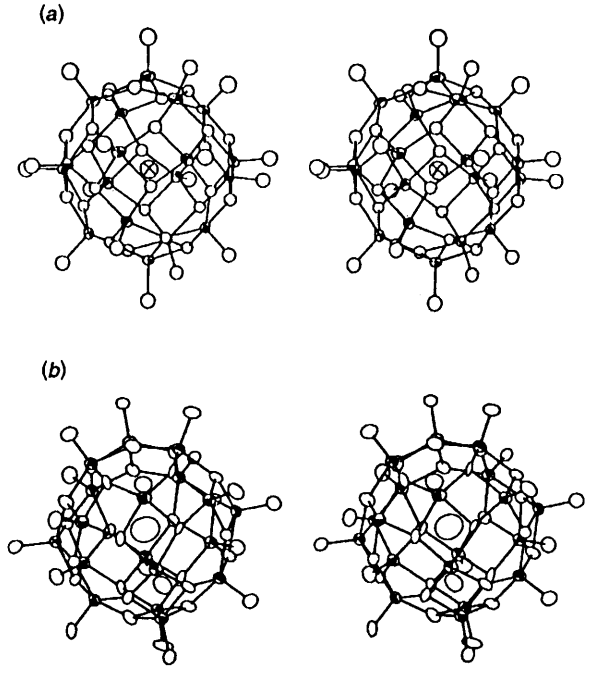

Fig. 3 Stereoscopic drawings of $[V_{18}O_{42}Cl]^{13-}$ (*a*) and $[V_{18}O_{42}(H_2O)]^{12-}$ (*b*). The central atoms are Cl and disordered water O(43), respectively

Spherical structure of $(VO)_{18}O_{24}X$ (X = Cl or H_2O) cage

The vanadium frameworks in clusters **1** and **2** are shown in Fig. 4. The central Cl atom in **1** [or O(43) in **2**] is approximately midway between the polar V(1) and V(2) atoms, being slightly displaced towards V(1) by 0.05(1) and 0.03(2) Å, respectively. The S_8 symmetry operation brings each V and O atom in the mean tetragonal V(3)–V(6) (neighbouring V–V–V angles almost 90°) and octagonal O(27)–O(34) (neighbouring O–O–O angles almost 135°) planes into near coincidence with each atom in the mean tetragonal V(7)–V(10) and octagonal O(35)–O(42) planes. The VO_5 square pyramids at polar V(1,2) centres share edges of corresponding pyramids at V(3)–V(6) and V(7)–V(10) with average V···V distances of 2.873(5) and 2.930(6) Å in **1** and **2**, respectively. The five mean planes of V(3)–V(6), O(27)–O(34), V(11)–V(18), O(35)–O(42) and V(7)–V(10) are almost parallel and each of the V(1,2,11,15) and V(1,2,13,17) mean planes intersects these five planes at an angle of about 90°. A set of two octagonal μ_3-O(27–34) and O(35)–O(42) planes is located about 1.25 Å above and below the central octagonal V(11)–V(18) plane (neighbouring V–V–V angles almost 135°) which is positioned 0.03 Å from Cl in **1** and 0.02 Å from O(43) in **2** towards V(2). Similarly, the tetragonal V(3)–V(6) and V(7)–

Table 1 Crystal and refinement data for clusters **1** and **2**

	1	**2**
Formula	$H_{26.5}ClK_{9.5}O_{53.5}V_{18}$	$H_{36}K_{10}O_{59}V_{18}$
M	2207	2288
Symmetry	Triclinic	Monoclinic
Space group	$P\bar{1}$	$P2_1/n$
a/Å	15.280(7)	12.793(8)
b/Å	18.841(5)	37.98(1)
c/Å	13.055(7)	12.614(6)
α/°	91.09(4)	
β/°	128.89(3)	97.13(4)
γ/°	94.09(4)	
U/Å^3	2908(5)	6081(4)
Z	2	4
D_c/g cm^{-3}	2.520	2.386
μ/cm^{-1}	35.765	34.111
F(000)	2132	4196
Crystal size/mm	0.3 × 1.0 × 0.03, plate	0.8 × 0.4 × 0.05, plate
Data collection range/°	$5 \leqslant 2\theta \leqslant 55$	$2 \leqslant 2\theta \leqslant 55$
hkl ranges	±20, ±25, 0–17	±17, 0–50, 0–17
No. data measured	13 999	14 816
No. unique data	13 405	14 197
No. observed data	6133 [$\|F\| \geqslant 3.0\sigma(F)$]	5392 [$\|F\| \geqslant 5.0\sigma(F)$]
No. variables	475	649
R	0.088	0.101
R'	0.107	0.123
Goodness of fit, S	2.87	3.78
Maximum shift/error	0.004	0.007

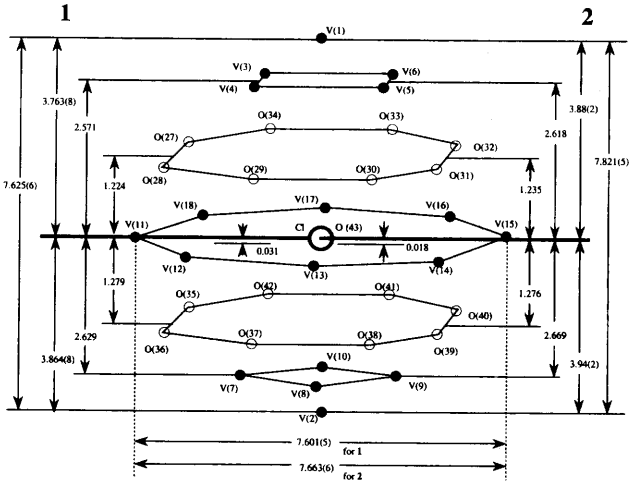

Fig. 4 Vanadium frameworks of the anions in clusters **1** and **2**. Average distances (Å) from the central octagonal V(11)–V(18) plane are given

V(10) planes are located about 2.60 Å in **1** and 2.64 Å in **2** above and below the central octagonal V(11)–V(18) plane. The distance [7.625(6) in **1** and 7.821(5) Å in **2**] between the two polar V(1) and V(2) atoms is slightly longer than the diagonal distance [average 7.601(5) in **1** and 7.663(6) Å in **2**] of the central octagonal V(11)–V(18) plane. Since the former corresponds to the inner axial diameter of the $V_{18}O_{42}$ shell and the latter to the inner equatorial one, the difference (0.02 in **1** and 0.16 Å in **2**) between the two distances indicates the distortion from a perfect sphere. However, the V_{18} clusters, $[H_{3.5}V_{18}O_{42}Cl]^{9.5-}$ and $[H_2V_{18}O_{42}(H_2O)]^{10-}$, are closer to a perfect sphere than is $[V_{15}O_{36}(CO_3)]^{7-}$, since the difference (1.632 Å) between the axial (5.549 Å) and equatorial (7.181 Å) distances for the V_{15} cluster $[H_2V_{15}O_{36}(CO_3)]^{7-}$ was larger.[1] The inner diameters of the V_{18} anion for **1** are (≈0.20 in the axial and ≈0.06 Å in the equatorial) smaller than for **2**. This can be explained in terms of the electrostatic attraction between the Cl^- and V^{IV} which results in weakening of the electrostatic repulsion between V^{IV} atoms compared with the case of the uncharged H_2O in **2**.

Magnetic susceptibility

The effective magnetic moment (μ_{eff}) was calculated from $\mu_{eff} = 2.828\ (\chi T)^{\frac{1}{2}}$.[17] The temperature dependences of the product χT for clusters **1** and **2** are shown in Fig. 5(*a*) and 5(*b*) respectively, where χ is the molar magnetic susceptibility and T the temperature. The room-temperature values of χT (2.27 emu K, $\mu_{eff} = 4.26\ \mu_B$ for **1** and 2.10 emu K, $\mu_{eff} = 4.10\ \mu_B$ for **2**), which are close to the values for six uncoupled electrons (2.25 emu K, $\mu_{eff} = 4.24\ \mu_B$), are much smaller than expected for 18 uncoupled $S = \frac{1}{2}$ spins (6.75 emu K, $\mu_{eff} = 7.35\ \mu_B$), indicative of antiferromagnetic coupling. Initially χT decreases gradually with decreasing temperature, down to about 1.7 (for **1**) and 1.4 (for **2**) emu K which are close to the value (1.50 emu K, $\mu_{eff} = 3.46\ \mu_B$) expected for four unpaired electrons, before decreasing rapidly below 50 K where they reach 0.6 and 0.3 emu K at 4.2 K. This may be indicative of the predominance of weak intramolecular antiferromagnetic exchange interactions at low temperature. A simple model for the magnetic behaviour of the V_{18} cluster takes into account antiferromagnetic couplings between vanadium centres bridged by two oxo groups, since the exchange pathways involving the V···V centres will be determined by two μ-oxo groups, with short distances; the antiferromagnetic coupling of $K_6[H_3KV_{12}As_3O_{39}(AsO_4)]\cdot 8H_2O$, $K_6[V_{15}As_6O_{42}(H_2O)]\cdot 8H_2O$ and $[NH_4]_6[V_{14}As_8O_{42}(SO_3)]$ has been discussed in detail.[18,19] Then, the strongest antiferromagnetic exchange pathway involving the V···V centres can be associated with the short V···V distances of ≤2.93 Å. This occurs with V(1)···V(6) [2.792(5)], V(2)···V(8) [2.847(5)], V(11)···V(12) [2.903(5)], V(13)···V(14) [2.914(5)], V(15)···V(16) [2.912(5)] and V(17)···V(18) [2.900(5)] for **1** and V(1)···V(4) [2.902(6)], V(2)···V(7) [2.913(6)], V(11)···V(12) [2.922(6)], V(13)···V(14) [2.924(6)], V(15)···V(16) [2.921(6)] and V(17)···V(18) [2.934(6) Å] for **2** and results in spin pairings for these six $V^{IV}\cdots V^{IV}$ pairs. Thus, at high temperature where the spins only within the V···V pairs with short distances of ≤2.93 Å are completely paired, six spins [at V(3–5,7,9,10)

Table 2 Atomic coordinates for clusters **1** and **2** with estimated standard deviations in parentheses

	1			**2**		
Atom	*x*	*y*	*z*	*x*	*y*	*z*
V(1)	0.4623(3)	0.2194(2)	−0.1021(3)	−0.0397(3)	0.1387(1)	−0.0071(3)
V(2)	1.0902(3)	0.2945(2)	0.2373(4)	0.2670(3)	0.1225(1)	0.5671(3)
V(3)	0.5145(3)	0.3189(2)	−0.2215(3)	0.1673(3)	0.1051(1)	0.0078(3)
V(4)	0.5453(3)	0.1264(2)	−0.2037(3)	−0.0806(3)	0.0753(1)	0.1095(3)
V(5)	0.6059(3)	0.1364(2)	0.1171(3)	−0.1459(3)	0.1688(1)	0.1658(3)
V(6)	0.5761(2)	0.3289(2)	0.1008(3)	0.0978(3)	0.1985(1)	0.0615(3)
V(7)	0.9431(3)	0.2777(2)	-0.0468(3)	0.2647(3)	0.0595(1)	0.4351(3)
V(8)	1.0106(3)	0.1471(2)	0.1936(3)	0.0404(3)	0.1034(1)	0.5461(3)
V(9)	1.0329(3)	0.2885(2)	0.4109(3)	0.1680(3)	0.1907(1)	0.5141(3)
V(10)	0.9680(3)	0.4191(2)	0.1721(3)	0.3919(3)	0.1469(1)	0.4023(3)
V(11)	0.6993(3)	0.2438(2)	−0.2734(3)	0.1773(3)	0.0358(1)	0.2148(3)
V(12)	0.7620(3)	0.1092(2)	−0.1528(3)	−0.0124(3)	0.0411(1)	0.3211(3)
V(13)	0.7962(3)	0.0552(2)	0.0777(4)	−0.1466(3)	0.1004(1)	0.3767(3)
V(14)	0.8520(3)	0.1225(2)	0.3177(3)	−0.1097(3)	0.1761(1)	0.4036(3)
V(15)	0.8283(3)	0.2624(2)	0.3932(3)	0.0415(3)	0.2272(1)	0.3299(3)
V(16)	0.8118(3)	0.4031(2)	0.2972(3)	0.2463(3)	0.2195(1)	0.2526(3)
V(17)	0.7335(3)	0.4519(2)	0.0427(3)	0.3618(3)	0.1618(1)	0.1658(3)
V(18)	0.7162(3)	0.3907(2)	−0.1757(3)	0.3475(3)	0.0848(1)	0.1736(3)
K(1)	1.0	0	0	0.5927(6)	0.1633(3)	−0.0378(6)
K(2)	1.2424(4)	0.4376(3)	0.5269(5)	0.6211(4)	0.1503(2)	0.2775(5)
K(3)	0.8641(5)	0.3760(3)	−0.3253(6)	0.4588(7)	0.2523(3)	0.0960(6)
K(4)	1.2698(5)	0.3529(4)	0.8257(6)	0.3484(5)	0.2589(2)	0.4943(6)
K(5)	0.6688(5)	−0.0448(3)	0.1912(6)	0.1457(5)	0.2989(2)	0.0881(6)
K(6)	0.5792(6)	−0.0633(4)	−0.2344(7)	−0.2492(5)	0.2456(2)	0.2870(5)
K(7)	1.1511(8)	0.4316(4)	0.0750(9)	0.1482(5)	−0.0240(2)	0.4616(5)
K(8)	0.2789(6)	0.1958(5)	0.5332(8)	0.2059(5)	0.0464(2)	0.7277(4)
K(9)	0.7355(8)	−0.0121(7)	−0.4408(7)	0.1350(6)	0.1580(2)	−0.2193(4)
K(10)	0.9187(8)	0.1593(6)	0.711(1)	−0.067(1)	0.0611(3)	−0.1694(6)
Cl	0.7728(6)	0.2599(4)	0.0706(7)			
O(1)	0.327(1)	0.2004(8)	−0.178(1)	−0.102(1)	0.1395(5)	−0.130(1)
O(2)	1.225(1)	0.3129(8)	0.310(2)	0.327(1)	0.1192(5)	0.691(1)
O(3)	0.399(1)	0.3415(7)	−0.351(1)	0.182(1)	0.0948(5)	−0.112(1)
O(4)	0.439(1)	0.0701(8)	−0.316(1)	−0.165(1)	0.0520(5)	0.031(1)
O(5)	0.529(1)	0.0794(7)	0.131(1)	−0.259(1)	0.1874(5)	0.124(1)
O(6)	0.484(1)	0.3602(7)	0.110(1)	0.089(1)	0.2283(5)	−0.030(1)
O(7)	1.017(1)	0.2919(8)	−0.098(1)	0.323(1)	0.0272(5)	0.502(1)
O(8)	1.117(1)	0.1015(8)	0.249(1)	0.013(1)	0.0915(5)	0.664(1)
O(9)	1.148(1)	0.3035(7)	0.562(1)	0.189(1)	0.2175(5)	0.617(1)
O(10)	1.052(1)	0.4892(8)	0.214(1)	0.513(1)	0.1532(5)	0.453(1)
O(11)	0.663(1)	0.2415(8)	−0.421(1)	0.206(1)	−0.0051(5)	0.186(1)
O(12)	0.763(1)	0.0446(8)	−0.237(2)	−0.057(1)	0.0026(5)	0.349(1)
O(13)	0.799(1)	−0.0294(8)	0.086(2)	−0.257(1)	0.0879(5)	0.415(1)
O(14)	0.885(1)	0.0648(8)	0.420(1)	−0.204(1)	0.1970(4)	0.453(1)
O(15)	0.852(1)	0.2636(8)	0.533(1)	0.006(1)	0.2679(5)	0.351(1)
O(16)	0.831(1)	0.4658(7)	0.396(1)	0.303(1)	0.2575(5)	0.241(1)
O(17)	0.717(1)	0.5340(8)	0.027(1)	0.466(1)	0.1766(5)	0.115(1)
O(18)	0.695(1)	0.4497(8)	−0.274(1)	0.449(1)	0.0638(5)	0.133(1)
O(19)	0.489(1)	0.2181(6)	−0.229(1)	0.021(1)	0.0934(5)	0.025(1)
O(20)	0.527(1)	0.1303(6)	−0.069(1)	−0.128(1)	0.1232(4)	0.096(1)
O(21)	0.546(1)	0.2269(7)	0.085(1)	−0.046(1)	0.1823(4)	0.068(1)
O(22)	0.498(1)	0.3201(7)	−0.087(1)	0.106(1)	0.1532(4)	0.001(1)
O(23)	1.020(1)	0.2181(7)	0.098(1)	0.178(1)	0.0821(4)	0.529(1)
O(24)	1.067(1)	0.2252(7)	0.325(1)	0.131(1)	0.1452(4)	0.566(1)
O(25)	1.047(1)	0.3576(7)	0.314(1)	0.299(1)	0.1658(4)	0.500(1)
O(26)	1.003(1)	0.3523(7)	0.091(1)	0.347(1)	0.1025(4)	0.460(1)
O(27)	0.605(1)	0.3084(7)	−0.276(1)	0.216(1)	0.0650(4)	0.101(1)
O(28)	0.628(1)	0.1597(7)	−0.266(1)	0.028(1)	0.0440(4)	0.177(1)
O(29)	0.675(1)	0.0744(7)	−0.098(1)	−0.125(1)	0.0721(4)	0.253(1)
O(30)	0.722(1)	0.0824(7)	0.144(1)	−0.168(1)	0.1431(4)	0.295(1)
O(31)	0.736(1)	0.1750(7)	0.296(1)	−0.080(1)	0.2006(4)	0.274(1)
O(32)	0.715(1)	0.3252(7)	0.283(1)	0.099(1)	0.2233(4)	0.200(1)
O(33)	0.672(1)	0.4117(6)	0.124(1)	0.248(1)	0.1935(4)	0.120(1)
O(34)	0.618(1)	0.4042(7)	−0.133(1)	0.298(1)	0.1243(4)	0.078(1)
O(35)	0.811(1)	0.3247(7)	−0.168(1)	0.304(1)	0.0589(4)	0.290(1)
O(36)	0.830(1)	0.1955(7)	−0.158(1)	0.139(1)	0.0393(4)	0.3574(9)
O(37)	0.884(1)	0.0968(7)	0.028(1)	−0.030(1)	0.0716(4)	0.439(1)
O(38)	0.927(1)	0.1024(7)	0.246(1)	−0.076(1)	0.1332(4)	0.483(1)
O(39)	0.943(1)	0.2109(7)	0.411(1)	0.022(1)	0.1990(4)	0.456(1)
O(40)	0.923(1)	0.3428(7)	0.400(1)	0.190(1)	0.2191(4)	0.384(1)
O(41)	0.872(1)	0.4431(7)	0.220(1)	0.354(1)	0.1851(4)	0.302(1)
O(42)	0.832(1)	0.4324(6)	0.002(1)	0.401(1)	0.1239(4)	0.264(1)

Table 2 (*continued*)

	1			2		
Atom	*x*	*y*	*z*	*x*	*y*	*z*
O(43)	1.051(1)	0.4084(8)	0.675(1)	0.112(2)	0.1322(7)	0.279(2)
O(44)	0.4601(9)	0.4569(6)	0.256(1)	0.546(1)	0.2256(5)	0.307(1)
O(45)	0.914(1)	−0.167(1)	0.319(2)	0.307(1)	0.0031(4)	0.997(1)
O(46)	1.400(1)	0.466(1)	0.810(2)	0.415(2)	0.1271(6)	−0.102(2)
O(47)	0.456(1)	0.3420(9)	0.459(2)	−0.199(2)	0.3028(7)	0.402(2)
O(48)	1.401(2)	0.474(1)	0.497(2)	0.295(2)	−0.0228(7)	0.779(2)
O(49)	0.671(2)	0.122(1)	0.448(2)	0.449(2)	0.3174(8)	0.189(2)
O(50)	1.094(2)	0.123(2)	−0.028(3)	0.733(2)	0.1860(9)	−0.161(2)
O(51)	0.646(2)	0.379(1)	−0.567(2)	0.637(2)	0.1041(8)	0.119(2)
O(52)	0.497(4)	−0.045(2)	−0.496(4)	0.443(2)	0.2074(7)	0.636(2)
O(53)	0.955(2)	0.026(1)	−0.348(2)	0.532(3)	0.011(1)	0.608(3)
O(54)	0.150(2)	0.089(1)	0.551(2)	0.096(3)	0.022(1)	0.911(3)
O(55)				0.692(3)	0.097(1)	−0.141(3)
O(56)				0.564(2)	0.0819(8)	0.524(2)
O(57)				0.277(4)	−0.056(1)	0.342(4)
O(58)				0.267(4)	0.366(1)	0.137(4)
O(59)				0.061(4)	0.372(1)	0.191(4)

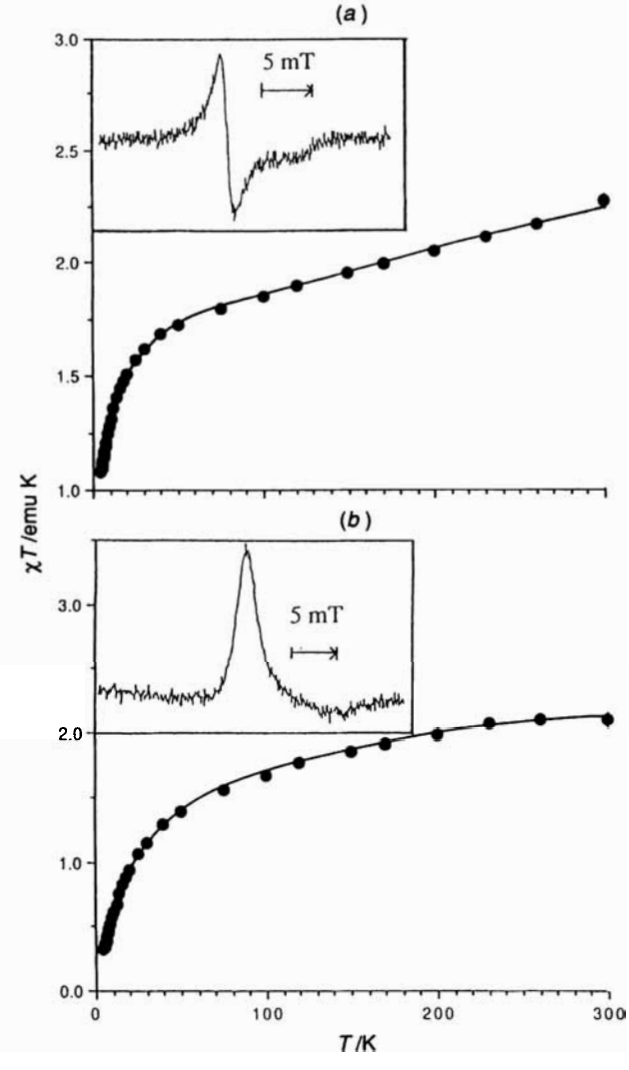

Fig. 5 Temperature dependence of χT for clusters **1** (*a*) and **2** (*b*). The inserts indicate the ESR spectra of the powdered samples at room temperature

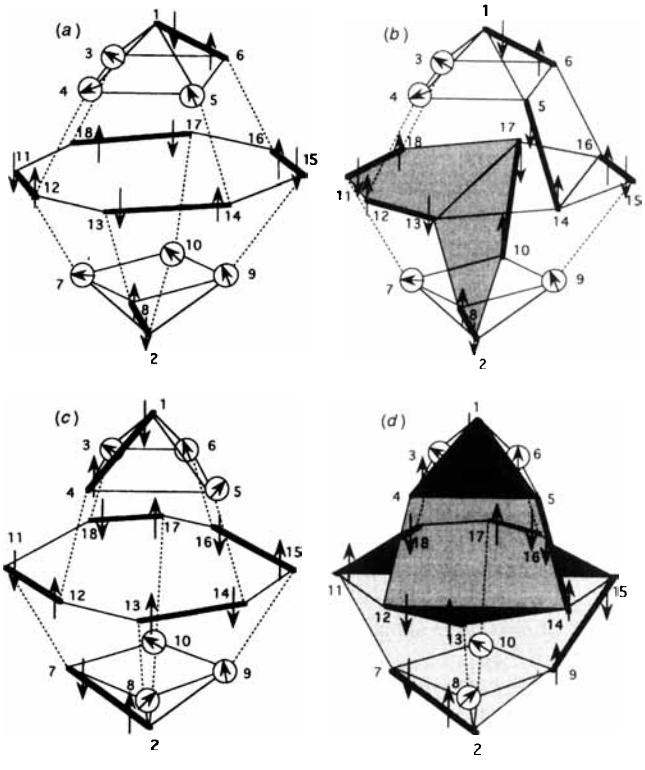

Fig. 6 Schematic spin arrangements preferred for six uncoupled [(*a*) and (*c*), at room temperature] and four uncoupled [(*b*) and (*d*), at low temperature] $S = \frac{1}{2}$ spins in clusters **1** [(*a*) and (*b*)] and **2** [(*c*) and (*d*)]. Numbers and bold lines denote the vanadium atoms and spin pairing in $V^{IV} \cdots V^{IV}$ pairs

centres in **1** and V(3,5,6,8–10) centres in **2**] left on the V(3)–V(6) and V(7)–V(10) planes are uncorrelated to provide the $S = 7$ spin state. Fig. 6 shows preferred spin orientations at vanadium centres in the $V^{IV}{}_{18}$ clusters **1** and **2**. The ESR spectra of powdered samples of **1** and **2** at room temperature showed (Fig. 5) broad signals due to axially distorted paramagnetic centres ($g_{\parallel} = 1.94$ and $g_{\perp} = 1.98$ with $\Delta H_{pp} = 1.82$ mT for **1** and $g_{\parallel} = 1.93$ and $g_{\perp} = 1.98$ for **2**) which are in good agreement with those ($g_{\parallel} = 1.93$ and $g_{\perp} = 1.98$) for three vanadium(IV) centres localized on the central triangular vanadium plane in the structure of $K_6[V^{IV}{}_{15}As_6O_{42}(H_2O)]\cdot 8H_2O$,[19,20] suggesting that three vanadium(IV) centres on each of the V(3)–V(6) and V(7)–V(10) planes are localized in a similar way to the spin orientation for the $V^{IV}{}_{15}As_6$ cluster, at room temperature [Fig. 6(*a*) and 6(*c*)] where the strong antiferromagnetic coupling is predominant. In the low-temperature range weak couplings occur in V(5)···V(14) [2.979(5)] and V(10)···V(17) [2.971(5)] for **1** and V(5)···V(14) [2.990(5)] and V(9)···V(15) [3.001(5)] for **2**, which are related to the slightly long V···V distances up to 3.00 Å. The occurrence of such

couplings in the anions induces complete couplings within the $V^{IV} \cdots V^{IV}$ pairs in both the extended-chair-configurated hexagon [V(1,5,14,15,16,6) in **1** and V(1,4,12,13,14,5) in **2**] and the folded octagon [V(2,8,13,12,11,18,17,10) in **1** and V(2,7,11,18,17,16,15,9) in **2**], defined by six and eight V^{IV} atoms, respectively. This leaves four vanadium(IV) centres in the V(3)–V(6) and V(7)–V(10) planes (two for each plane) largely uncoupled to provide the $S = 5$ spin state [Fig. 6(*b*) and 6(*d*)]. We interpret the temperature dependence of χT in the range 70–250 K as indicating a mixture of two spin states, $S = 7$ and 5. Thus, the intermediate spin state $S = 6$ is formally observed at 100–150 K (Fig. 5), if the contribution of $S = 5$ increases with decreasing temperature. The $V^{IV} \cdots V^{IV}$ distances responsible for the $V^{IV} \cdots V^{IV}$ spin pairing in **1** are shorter than in **2**, indicating that the lack of correlation of the spins left behind after antiferromagnetic coupling would be stronger in **1**, resulting in a larger contribution of the $S = 7$ state. This is reflected in the larger values of χ for **1**, compared with **2**. The shift of the V–O–V vibrational stretching bands to slightly higher wavenumbers (≈ 5 cm^{-1}) for **1** is also in accord with the shorter $V^{IV} \cdots V^{IV}$ distances in **1**, compared with those for **2** (Fig. 1).

Acknowledgements

We acknowledge a Grant-in-Aid for Scientific Research, no. 06403011, from the Ministry of Education, Science, Sports and Culture for support of this work.

References

1 Part 1, T. Yamase and K. Ohtaka, *J. Chem. Soc., Dalton Trans.*, 1994, 2599.
2 A. Müller, M. Penk, R. Rohlfing, E. Krickemeyer and J. Döring, *Angew. Chem., Int. Ed. Engl.*, 1990, **29**, 926.
3 V. W. Day, W. G. Klemperer and O. M. Yaghi, *J. Am. Chem. Soc.*, 1989, **111**, 5959.
4 A. Müller, M. Penk, E. Krickemeyer, H. Bögge and H.-J. Walberg, *Angew. Chem., Int. Ed. Engl.*, 1988, **27**, 1719.
5 A. Müller, E. Krickemeyer, M. Penk, H.-J. Walberg and H. Bögge, *Angew. Chem., Int. Ed. Engl.*, 1987, **26**, 1045.
6 A. Müller, E. Krickemeyer, M. Penk, R. Rohlfing, A. Armatage and H. Bögge, *Angew. Chem., Int. Ed. Engl.*, 1991, **30**, 1674.
7 A. Müller, R. Rohlfing, K. J. Döring and M. Penk, *Angew. Chem., Int. Ed. Engl.*, 1991, **30**, 588.
8 G. K. Johnson and E. O. Schlemper, *J. Am. Chem. Soc.*, 1978, **100**, 3465.
9 P. Román, A. San José, A. Luque and J. M. Gutiérrez-Zorrilla, *Inorg. Chem.*, 1993, **32**, 775.
10 C. J. O'Conner, *Prog. Inorg. Chem.*, 1982, **29**, 203.
11 G. J. Gilmore, *J. Appl. Crystallogr.*, 1984, **42**, 46.
12 N. Walker and D. Stuart, *Acta Crystallogr., Sect. A*, 1983, **158**, 3.
13 TEXSAN, Single-crystal structure analysis software, Molecular Structure Corporation, The Woodlands, TX, 1989.
14 I. D. Brown and K. K. Wu, *Acta Crystallogr., Sect. B*, 1976, **32**, 1957.
15 J. Emsley, *Chem. Soc. Rev.*, 1980, **9**, 91.
16 R. D. Shannon, *Acta Crystallogr., Sect. A*, 1976, **32**, 751.
17 D. N. Hendrickson, Y. S. Sohn and H. B. Gray, *Inorg. Chem.*, 1971, **10**, 1559.
18 A. L. Barra, D. Gatteschi, L. Pardi, A. Müller and J. Döring, *J. Am. Chem. Soc.*, 1992, **114**, 8509.
19 A. L. Barra, D. Gatteschi, B.-S. Tsukerblatt, J. Döring, A. Müller and L.-C. Brunel, *Inorg. Chem.*, 1992, **31**, 5132.
20 D. Gatteschi, L. Pardi, A. L. Barra, A. Müller and J. Döring, *Nature (London)*, 1991, **354**, 463.

Received 19*th June* 1995; *Paper* 5/03958D